Last but not least, much more objective activity figures may be gained by video techniques, which were not available in 1966. These can be used to calibrate visual estimates, too. We hope that in 2032, Leonid observers in their preparation can rely on more accurate figures from the hopefully high EZHRs of the 1998 and 1999 Leonid returns.

Acknowledgments

We thank the observers who contributed their scores to this study. Jürgen Rendtel made a number of helpful comments, and André Knöfel made valuable suggestions to improve the RMS software. Lars Winter helped in a literature search for observational material of 1866 and 1966 in the catacombs of Bergedorf Observatory's library. He and the first author wish to acknowledge funding by the U. Wagner Foundation, grant no. 112/93-02.9/1.

References

[1] J. Rendtel, R. Arlt, A. McBeath (eds.), "Handbook for Visual Meteor Observers", IMO Monograph No. 2, 1996, p. 240.
[2] J. Rao, "The Leonids: King of Meteor Showers", *Sky and Telescope* 90, 1995, pp. 24–31.
[3] J. Ashbrook, "Great Leonid Meteor Shower of 1966", *Sky and Telescope* 33, 1967, pp. 89–92.
[4] J. Rendtel, R. Arlt, "Perseids 1995 and 1996—An Analysis of Global Data", *WGN* 24, 1996, pp. 141–147.
[5] P. Jenniskens, "Meteor Stream Activity II. Meteor Outbursts", *Astron. Astroph.* 295, 1995, pp. 206–235.
[6] M. Langbroek, in "Letters to WGN," *WGN* 24, 1996, pp. 2–4.
[7] J. Rendtel, in "Letters to WGN," *WGN* 24, 1996, pp. 4–5.
[8] S. Molau, in "Letters to WGN," *WGN* 24, 1996, p. 129.
[9] C. Verbeeck, in "Letters to WGN," *WGN* 24, 1996, p. 130.
[10] S. Molau, "New Results from Video Meteor Observations", *WGN* 23, 1995, pp. 217–224.
[11] B.A. Smith, in "Letter to Sky and Telescope," *Sky and Telescope* 91, 1996, pp. 8–9.
[12] G.B. Airy, "Inference from the Observed Movement of the Meteors in the Appearance of 1866, November 13-14", *Monthly Notices of the Royal Astronomical Society* 27, 1866, p. 56.
[13] W.R. Dawes, "On the Meteor Shower of 1866, Nov. 12–14", *Monthly Notices of the Royal Astronomical Society* 27, 1866, pp. 46–50.

Revisiting the Radio Doppler Effect from Forward-scatter Meteor Head Echoes

James Richardson and Werfried Kuneth

Following an introduction to the radio meteor head echo and its historical aspects, a PC-based technique is described whereby the radio Doppler effect from meteor head echoes can be used to make rough meteor range and speed measurements, employing a commercial AM or CW transmitter in a forward-scatter link. The technique is then applied to four known shower meteors, two Leonid and two Geminid, which provided measurable head echoes in addition to specular trail reflections.

1. Introduction

On the night of November 17, 1996, the Leonid meteor shower produced a noteworthy display for both visual and radio meteor observers. While only reaching typical major shower strength as far as rates were concerned, the shower was enjoyably rich in swift, bright meteors and fireballs, some

producing enduring visual trains. For the radio observer, the shower produced an abundance of extremely strong, long-duration trail echoes, which occasionally overlapped with each other. It was also noticed by the authors that, while the Leonid radiant was relatively low in the sky, a higher-than-usual number of impressive meteor head echoes could also be heard, occurring just prior to the specular trail reflections. A repeat performance of this unusual radio display in 1997 prompted us to investigate the head echo phenomenon further.

The meteor head echo is a radio wave reflection from an apparent plasma cloud directly around the moving meteoroid as it plows through the upper atmosphere [1,2]. This is a separate phenomenon from the more common specular reflection from the meteor's trail [1,3] Over the 50 or so years of radio meteor research, there have been numerous explanations suggested for this plasma cloud's origin [3–6], but the production and detection mechanism still is uncertain. Investigations of this phenomenon continue today, using sophisticated, high-powered VHF and UHF meteor radars [7,8].

In the conventional back-scatter or forward-scatter system, this dense cloud of free electrons about the meteoroid presents a "moving ball" type of target to the radio waves from the transmitter, creating a very distinct Doppler-shifted signal at the receiver. In a Continuous Wave (CW) receiver, the meteor head echo sounds like a sharp, rapidly descending "whistle," just prior to the specular trail reflection and usually lasting less than half a second. Because significant head echoes are generated only by the brighter meteors having a favorable geometry, they can be rather elusive, occurring in about 0.1% of the trail echo population for a typical system [3]. Nonetheless, their significance as a reflected signal from a rapidly moving target was recognized as early as the late 1930s. This helped to bolster the gathering evidence in support of radio wave reflections from meteors (or their trails—under scientific debate at that time [1]).

McKinley [1] cites one of the first professional studies of this phenomenon:

> *"A novel aspect of the meteoric reflections was described by two Indian radio engineers, Chamanlal and Venkataraman* [9]. *They found that, when listening to a radio receiver tuned to an unmodulated short-wave transmitter, audible whistles could be heard which were short-lived and usually descending in pitch. This "radio Doppler effect" was correctly interpreted as a heterodyne beat between the transmitted wave and the wave reflected from a moving target. However, they assumed that the descending pitch of the beat note was due entirely to rapid retardation of the meteor whereas, as Appleton and Naismith* [10] *have pointed out, the effect should properly be construed as due to the change in apparent radial velocity that is observed when the meteor is moving with a relatively constant linear velocity across the observer's line of sight."*

At Stanford, Manning [11] became the first professional to work out the geometry, interference pattern, and resulting Doppler signal from such a moving ball target for the purpose of obtaining meteor speeds from meteor head echoes [3]. By that time, however, a different range-time method for obtaining meteor speeds had successfully been employed by Hey, Parsons, and Stewart [12] during the great Giacobinid shower of 1946. This became the first professional determination of meteor speeds using radio methods. Due to the rarity of appropriate meteor head echoes and the nearly exclusive use of pulse-type radar instruments by the professionals, the technique of measuring meteor speeds using the CW head echo Doppler shift was quickly abandoned for more practical methods [3]. McKinley [1] does mention the method as a viable and sensitive technique for use with CW systems, and it was this aspect that interested us. The meteor head echo represented a unique opportunity for advancing our amateur efforts in utilizing radio techniques for meteor studies.

2. Equation development

The first step in investigating the meteor head echo is to derive the relationship between the observed Doppler shift and the line-of-sight (radial) speed of the meteor. In the case of the moving target, two separate Doppler shifts occur: the first between the transmitter and the

meteor head, and the second between the meteor head and the receiver. Because we choose only to analyze those meteors which also cause a forward-scatter trail reflection, we know that the meteor path must lie within a plane which is orthogonal to the radio signal plane of propagation at the specular reflection point [1]. However, we lack specific information about the orientation of the meteor path within that plane. We therefore need to make the simplifying assumption that the radial speed between meteor and transmitter is the same as the radial speed between meteor and receiver. In essence, this reduces the forward-scatter situation to the back-scatter condition. This assumption is also aided by the observation that if the meteor path is oriented such that one radial speed is increased, it will cause a corresponding decrease in the opposite radial speed, partially canceling the effect of the orientation. Proceeding forward, the first Doppler shift between transmitter and meteor is given by

$$f_1 = \frac{c + v_\ell}{c} f_0,$$

where f_0 is the transmitter frequency (Hz), f_1 the frequency received at the meteor head (Hz), c the speed of light(299 792.458 km/s), and v_ℓ the line-of-sight (radial) speed (km/s). Now, we extend the signal from the meteor head down to the receiver to obtain

$$f_2 = \frac{c}{c - v_\ell} f_1,$$

where f_2 is the frequency received at the receiver (Hz). These are the standard equations first for a moving receiver, and then for a moving transmitter [13]. Combining and simplifying these two equations yields

$$f_2 = \frac{c + v_\ell}{c - v_\ell} f_0$$

or

$$\frac{v_\ell}{c} = \frac{f_2 - f_0}{f_2 + f_0}.$$

For the sum term in the above equation, the received frequency is equal to the transmitter frequency up to four significant digits. This gives us a final Doppler shift equation of

$$\Delta f = f_2 - f_0 = 2 \frac{v_\ell}{c} f_0$$

or a line-of-sight (radial) speed equation of

$$v_\ell = \frac{\Delta f}{2 f_0} c. \tag{1}$$

Note that if the meteor head is approaching the receiver, the Doppler shift Δf will be positive, and the line-of-sight speed v_ℓ will be positive. If the meteor head is receding from the receiver, the Doppler shift will be negative, and the line-of-sight speed will be negative.

The next step is to investigate the head echo geometry. Figure 1 shows a target moving perpendicularly across the field of view of a receiver. Initially, the line-of-sight distance between target and receiver is large, but decreases as the target approaches. This line-of-sight distance will continue to decrease until it passes through a minimum value at the point of closest approach (PCA) for the target. Note that at the PCA, the line-of-sight is at a right angle to the target's path. Following PCA passage, the line-of-sight distance will begin to increase again as the target recedes.

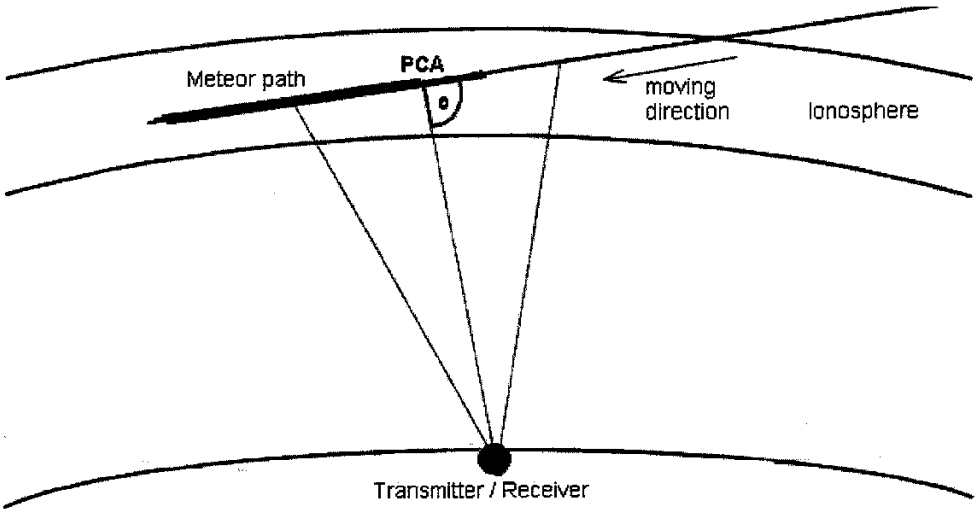

Figure 1 – A target moving across the field of view of a receiver. Radial lines indicate the line-of-sight at various points, including the point of closest approach (PCA).

Still using Figure 1, we next place transmitter and receiver together at the same location (back-scatter condition), with the radio signal path to and from the target following a line-of-sight (radial) path. The speed of the target is then split into two components: a radial component and a tangential component. The Doppler shift imparted by the target on the transmitted frequency becomes a function of the target's radial speed. For an approaching target, the radial speed will begin at some high value, with a corresponding high positive Doppler shift. As the target approaches the PCA, its radial speed will continuously decrease, creating a continuously decreasing Doppler shift. At PCA passage, the radial speed will pass through zero, with a corresponding Doppler shift of zero. All of the target's speed will be tangential to the line-of-sight, and the received frequency will equal the transmitted frequency. Following PCA passage, the radial speed will become increasingly negative, with an increasing negative Doppler shift. Thus, as the target approaches, passes through the PCA, and then recedes, the receiver will see a continuously decreasing frequency: first above the base frequency as the target approaches, equal to the base frequency at the PCA, and then below the base frequency as the target recedes.

Figure 2 shows the extension of Figure 1 to the forward-scatter condition, in which a meteor is moving between transmitter and receiver. With respect to the receiver, the meteor head will again display the same behavior as in Figure 1: it will approach the receiver at some radial speed, pass through a point of closest approach (PCA), and then recede. At the PCA, the radio reflection path will be at a right angle to the meteor's flight path, the radial speed will be zero and the Doppler shift will be zero. This allows us to set up a right triangle with the PCA-receiver line as the base (called r_0, for minimum range), the meteor's flight path as the perpendicular (m), and the line-of-sight (ℓ) at some other selected point forms the hypotenuse (all km). This yields the following relationship:

$$\ell^2 = r_0^2 + m^2.$$

If we assume the meteor to be traveling at a constant speed, then the above can be expanded to

$$\ell^2 = r_0^2 + (v_\mathrm{m}\Delta t)^2, \tag{2}$$

where v_m is the meteor speed (km/s), $\Delta t = t - t_0$ (s), t is the time of selected line-of-sight range (s), and t_0 is the time of PCA passage (s).

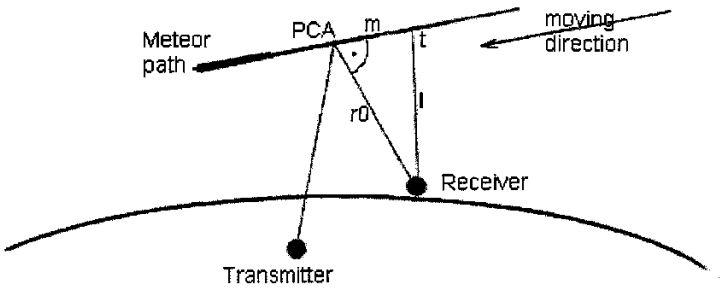

Figure 2 – In a forward-scatter link, a right triangle can be established between the receiver, the meteor's point of closest approach (PCA), and a selected meteor range at time t.

Note that this is the well-known hyperbolic equation used to solve for meteor speed using range-time information from a back-scatter radar [3]. For our purposes we are interested in the related rates for this triangle. Holding r_0 constant and differentiating with respect to time, yields

$$2\ell \frac{d\ell}{dt} = 2m\frac{dm}{dt},$$

or

$$\ell v_\ell = m v_\mathrm{m}.$$

Since $\ell^2 = r_0^2 + m^2$ and $m = v_\mathrm{m}\Delta t$, squaring both sides and expanding the ℓ and m terms yields

$$v_\ell^2 r_0^2 + v_\ell^2 v_\mathrm{m}^2 \Delta t^2 = v_\mathrm{m}^4 \Delta t^2.$$

We can then algebraically solve this equation for each of the desired terms:

- If Δt, v_ℓ, and v_m are known, we can solve for the PCA range r_0 as follows:

$$r_0 = v_\mathrm{m}\Delta t\sqrt{\frac{v_\mathrm{m}^2}{v_\ell^2} - 1}\,. \tag{3}$$

- If Δt, v_ℓ, and r_0 are known, then we can solve for the meteor speed v_m as follows:

$$v_\mathrm{m} = \sqrt{\frac{v_\ell}{2}\left(v_\ell + \sqrt{v_\ell^2 + \frac{4r_0^2}{\Delta t^2}}\right)}\,. \tag{4}$$

- Finally, we can solve for the expected Doppler frequency shift Δf for a given PCA range r_0, meteor speed v_m, and base frequency f_0 by substituting in equation (1) the solution for the line-of-sight (radial) speed v_ℓ:

$$\Delta f = -\,\mathrm{sgn}(\Delta t)\sqrt{\left(\frac{2f_0}{c}\right)^2 \frac{v_\mathrm{m}^2}{\frac{r_0^2}{v_\mathrm{m}^2\Delta t^2} + 1}}\,, \tag{5}$$

where $\mathrm{sgn}(\Delta t) = |\Delta t|/\Delta t$ is used to give the correct algebraic sign to Δf. Prior to the PCA, Δf will be positive, and after PCA, Δf will be negative.

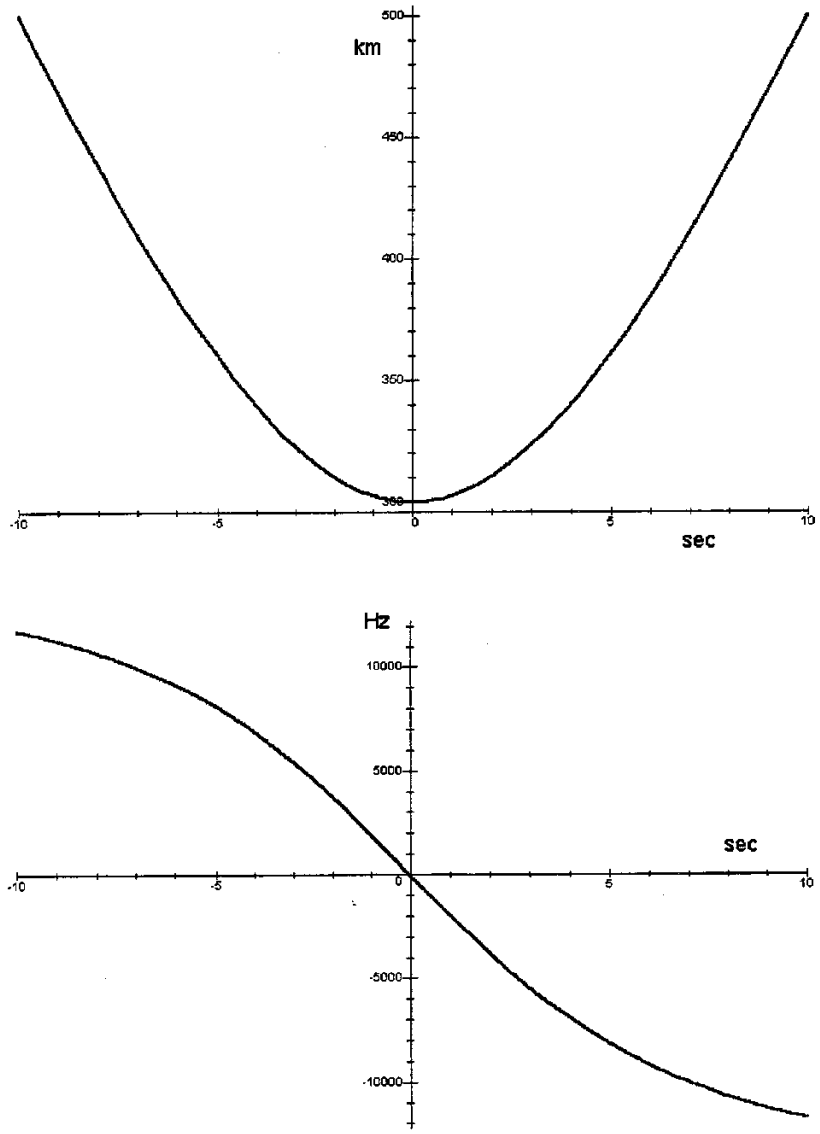

Figure 3 – Within a 10-second time window, the (*top*) hyperbolic range (km) versus time (s) plot, and (*bottom*) Doppler frequency shift Δf (Hz) versus time (s) plot for a "typical" forward scatter meteor head echo are shown. Note the curvilinear nature of the latter.

In order to demonstrate the predicted behavior of a meteor head echo using this last equation, we choose as "typical" values a range of $r_0 = 300$ km, a meteor speed of $v_m = 40$ km/s, and a transmitter operating frequency of $f_0 = 55.260$ MHz. Figure 3 shows the (*top*) hyperbolic range versus time plot using equation (2), and the (*bottom*) Doppler frequency shift versus time plot using equation (5). This figure has the relatively large time window of approximately 10 seconds in order to show the curvilinear nature of the frequency shift curve (equation (5)). If the frequency shift plot is extended to either left or right, the curve becomes asymptotic to a maximum frequency shift given by

$$\Delta f = \pm 2 \frac{v_m}{c} f_0.$$

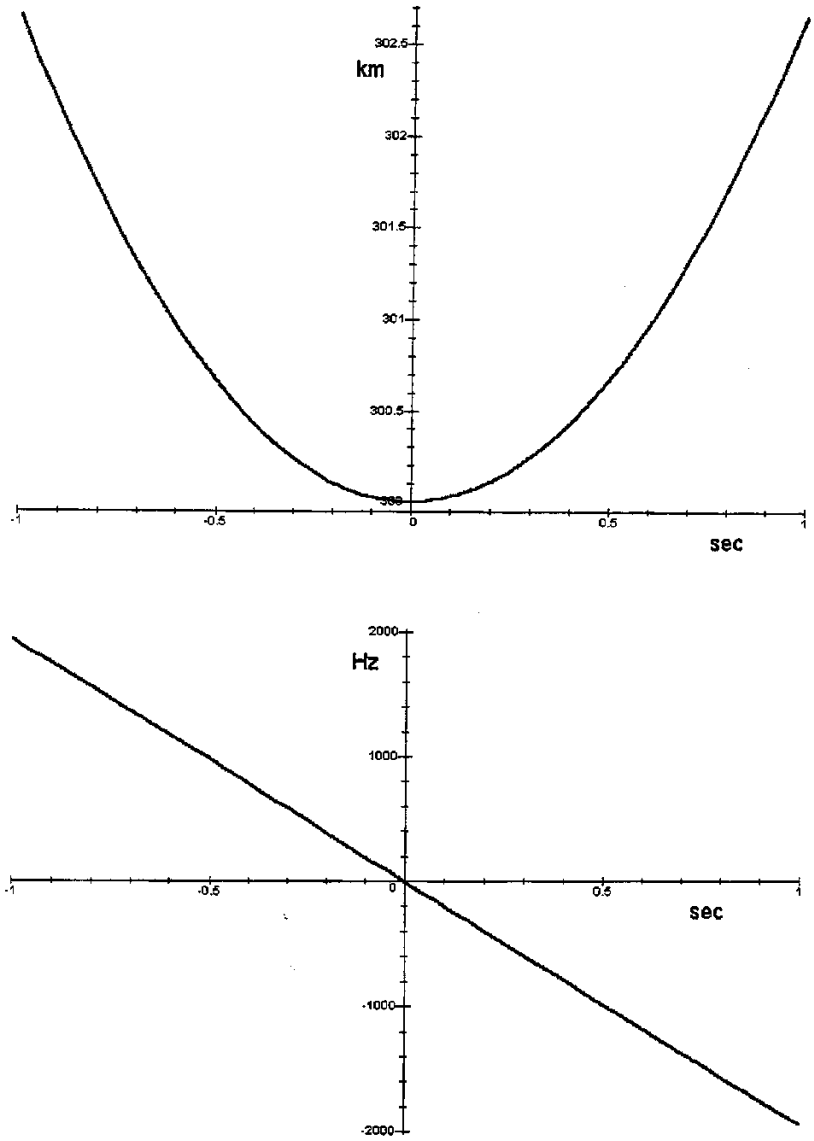

Figure 4 – Within a 1-second time window, the (*top*) hyperbolic range (km) versus time (s) plot, and (*bottom*) Doppler frequency shift Δf (Hz) versus time (s) plot for a "typical" forward scatter meteor head echo are shown. Note the linear nature of the latter over this limited time range.

For our "typical" meteor, the horizontal asymptotes for the frequency shift curve are located at ± 14.75 kHz. In practice, however, these limits are never encountered, since most meteor head echoes occur within half a second or so of the PCA. Figure 4 shows these same two equations over the more useful time range of approximately 1 second. Note that over this time span, the frequency shift curve is essentially linear, has a negative slope, and passes through 0 Hz of frequency shift as the meteor passes through the PCA range of 300 km. Faster meteor speeds will create a steeper slope, while slower meteors will create a shallower slope. In like fashion, meteors at a closer range will create a steeper slope, while meteors at a farther range will create a shallower slope. Of these two variables, the speed term is dominant, having a greater overall effect than the range term.

3. Analysis technique

From the above discussion, it becomes obvious that the most important point in the geometry is the point of closest approach (PCA) for the meteor head. Thus, in order to utilize these equations, proper identification of the PCA becomes paramount in order to solve for the other variables. It is also obvious from Figures 3 and 4 that the Doppler frequency shift versus time curve for a particular head echo cannot be used for this task because the curve passes linearly through the PCA (and base frequency) without inflections. Luckily, however, the base frequency, and hence the PCA, can be identified through another source: the specular reflection from the meteor trail. The meteor trail provides a relatively stationary target, which reflects the transmitter frequency to the receiver with very little to no Doppler shift. Upper-atmospheric winds can cause a trail reflection to have a "body-Doppler" of up to about 10–20 Hz [1], but for our purposes this is near the limits of our measurement accuracy and can be neglected. Hence, the PCA for the head echo is indicated when the head echo frequency matches the trail echo frequency. Using this point in time and frequency as our PCA reference point, our right triangle geometry can be utilized.

The data for this study was collected using the forward-scatter receiving stations located in Poplar Springs, Florida (J. Richardson) [14] and Ferndorf, Austria (W. Kuneth) [15]. Each station utilizes distant commercial television transmitters (AM mode, video carrier signals) as the forward-scatter signal source, within the 52–56 MHz frequency range. Commercial FM transmitters could not be utilized for this study, due to their lack of a frequency stable carrier signal. While both systems feed their receiver outputs to computerized data collection systems, the data collection systems were not used for this study. Instead, good quality audio recordings were made directly at the receivers during periods of known meteor shower activity. Each receiver was placed in CW mode, such that the recorded audio signal became the heterodyne beat frequency between the received frequency and a constant, internal BFO frequency (BFO = Beat Frequency Oscillator). The output frequency is given by

$$f_{\text{audio}} = f_2 - f_{\text{BFO}}.$$

This frequency downshift not only allowed us to monitor, by ear, incoming meteor head and trail echoes, but also to utilize audio recording equipment and analysis software. Because our receiver bandwidths are about 4–6 kHz, the audio signals recorded were generally on the order of 100 to 3000 Hz, depending upon the exact BFO setting in relation to the transmitter frequency.

The audio recordings at Poplar Springs were made using a Sony TCM-4000 mono-channel cassette tape recorder, which has a low noise, and relatively flat frequency response up to 15 kHz using FeO_2 tapes. Selected portions of the audio recordings were then digitized at 22 kHz using a SoundBlaster 16-bit ISA bus card and the Windows 95 sound recorder application, using the PCM format. A similar procedure was followed at Ferndorf.

Once digitized, audio spectrograms for the recordings were produced using the Spectrogram 2.3 software package [16]. This application is available as free-ware from the developer, and can be downloaded at various locations on the Internet. Spectrogram uses a Fast Fourier Transform (FFT) routine to produce an audio frequency versus time display for the recording having audio frequency plotted on the ordinate, time plotted on the abscissa, and signal strength indicated by either a color scale or a grey scale. For our selected audio recordings, a 2048 point FFT generally yielded the best results for the resolution given below:

Sample frequency (f): 22 000 Hz;
Frequency range ($f/2$): 0 Hz to 11 000 Hz;
FFT points (n): 2048;
Frequency divisions in range ($n/2$): 1024;
Frequency resolution: 11 Hz;
Frequency accuracy: ±5.5 Hz;
Time resolution: 4 ms (milliseconds);
Time accuracy: ±2 ms.

Spectrogram 2.3 provides a direct readout for the frequency and time of a point selected on the display using the mouse cursor. For each meteor head echo analyzed, as many measurements as could be practically taken were made along the line of the head echo, with the identification of the PCA (our reference point) being the most critical. As a general rule, measurements were not usually made within 50 ms of the PCA because such points usually displayed erratic (outlier) behavior due to measurement accuracy affects on the difference terms (Δf and Δt).

Using these measurements, the line-of-sight (radial) speed v_ℓ for the meteor could be calculated using equation (1). This result could also be applied to equations (3) and (4), provided that assumptions were made for one of the unknown variables. This points out the weakest part of this technique: without specific PCA range information, the meteor speed cannot be determined with accuracy, or without specific meteor speed information, the meteor range cannot be determined with accuracy. Despite the lack of accuracy, we nonetheless found it interesting to explore these areas, although the calculated values should be treated with a grain of skepticism.

In order to determine meteor PCA ranges, we purposely selected time periods in which a major meteor shower was at its peak and the radiant for the shower was passing through an altitude of about 20°–45°—biasing the collected recordings strongly toward particular shower members. Observations of previous major showers had also indicated that meteor head echo activity was noticeably enhanced with the shower radiant at low altitudes. We also desired that the shower radiant be as nearly perpendicular in azimuth to the forward-scatter link azimuth as could be achieved, in order to match our derived geometry as closely as possible, and to restrict the meteor reflection area to near the link "hot spot" locations. In the case of the Leonids, the distinctly characteristic head and trail echoes from this shower also helped to ensure a reasonably positive identification. Meteor speed assumptions were then taken from Cook's working list [17], and meteor PCA range assumptions were calculated using a simple forward-scatter "hot spot" model developed by Richardson using Maple (version 4.00C, 1996).

4. Data analysis

We now show the analysis of four recorded meteor head echoes: two Leonid echoes and two Geminid echoes.

Leonid head echo 1

Date: November 17, 1997;
Time: 08^h00^m UT (02^h00^m LT);
Radiant altitude: 35°;
Radiant azimuth: 83°.

Most probable link: Poplar Springs, FL - Baltimore, MD;
Link distance: 1230 km;
Link bearing: 38° (from receiver);
Relative radiant bearing: 45°;
Transmitter frequency (f_0): 55 260 490 Hz.

Figure 5 shows the audio spectrogram for Leonid 1. The meteor head echo is shown by the nearly linear sweep from 878 Hz at 442 ms to 264 Hz at 670 ms (the PCA), for a total sweep of 614 Hz in 228 ms. At this point, the much stronger, horizontal trail reflection begins, extending to the right off the screen and lasting for 5 seconds. With the beginning of the trail echo, the AGC for the receiver was triggered, reducing the gain and swamping out any further signal from the head echo.

Usually, the PCA and the beginning of the trail echo correspond quite close to each other, giving us three types of events: (*i*) if the trail echo begins prior to PCA passage, the head echo will be swamped prior to reaching the base frequency, making this type unusable; (*ii*) most commonly, the PCA and trail echo beginning are coincidental, similar to the back-scatter condition and matching our desired geometry most closely; and (*iii*) if the trail echo begins after PCA passage, the head echo can be followed below the base frequency. This last happens only rarely, however.

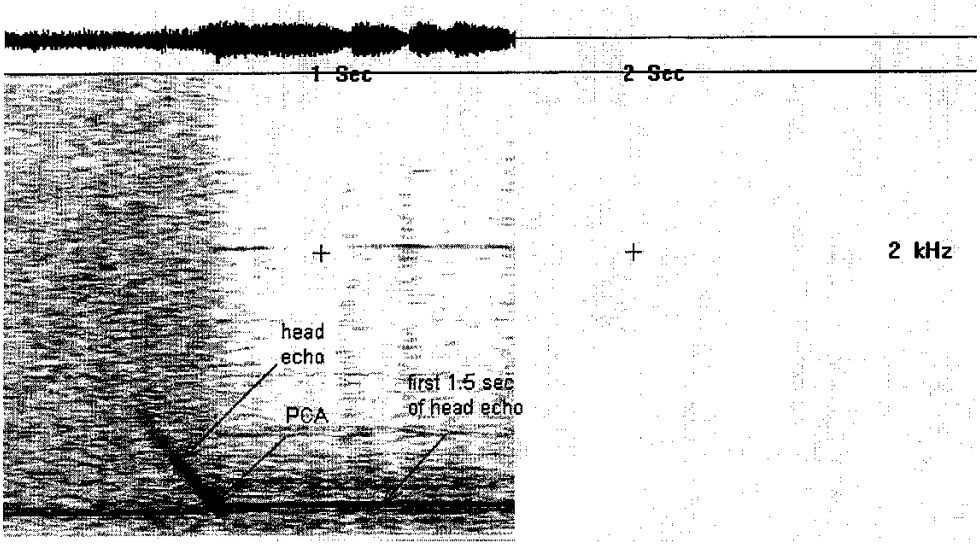

Figure 5 – Audio spectrogram for Leonid meteor recorded at Poplar Springs, Florida, on November 17, 1997, at 8^h00^m UT.

Table 1 – Data table for Leonid 1

Data point	Δf ±11 Hz	Δt ±4 ms	Slope Hz/ms	v_ℓ km/s	r_0 km	v_m km/s
1	614	−228	−3.58	1.67	684	68.3
2	571	−216	−3.25	1.55	697	67.6
3	506	−196	−3.07	1.37	714	66.8
4	420	−168	−2.67	1.14	737	65.8
5	356	−144	−2.32	0.966	745	65.4
6	291	−116	−2.69	0.789	734	65.9
7	205	− 84	−2.21	0.556	755	65.0
8	130	− 50	−2.60	0.353	709	67.1

PCA point: 264 Hz at 670 ms.

Using an assumed meteor speed of 70.7 km/s:

$\overline{r_0}$ = 722 km;
SD = 24.8 km;
Final PCA range: (722 ± 50) km (confidence interval = 2 × SD).

Using an assumed PCA range of (638 ± 200) km:

$\overline{v_m}$ = 66.5 km/s;
SD = 1.2 km/s;
Final v_m: (66.5 ± 10.8) km/s (confidence interval based upon high/low method for a range assumption accuracy of ±200 km. The selection of this accuracy is rather arbitrary, but is based upon encompassing the majority of the primary reflection area for the link).

An interesting facet of the data table is the apparent deceleration of the meteor over its flight path (m) of about 16 km. This can also be seen as a small change in the slope of the head echo line in Figure 5, making it slightly concave upward. Whether this is a true indication of meteor deceleration, or simply an effect of geometry not adequately covered in our assumptions, we cannot say at this point.

It should also be remembered that the two final results above cannot be used together, because each depends upon an assumption made in the other variable. These simply represent two possible fits to the same data, and of the two, we have more confidence in the range determination (based upon the classical Leonid speed) than in the meteor speed determination.

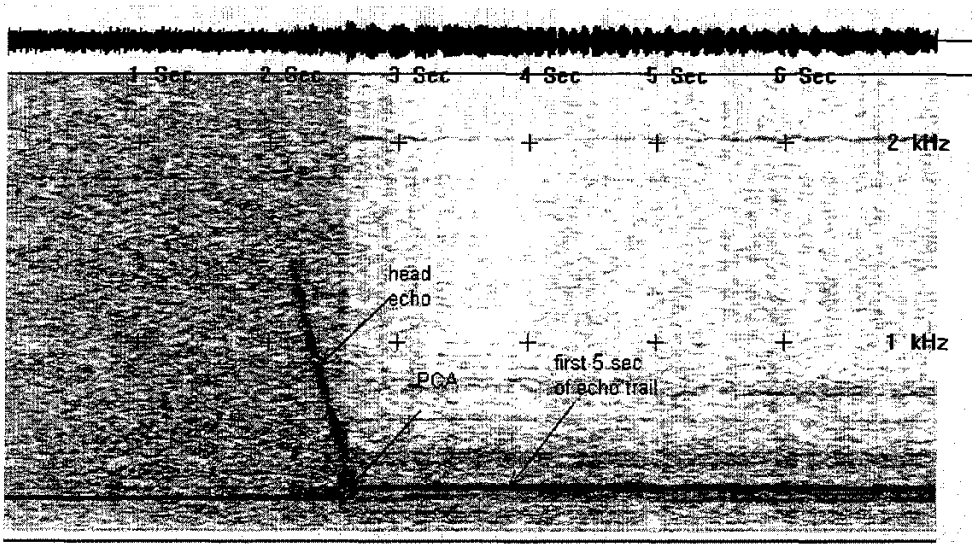

Figure 6 – Audio spectrogram for Leonid meteor recorded at Poplar Springs, Florida, on November 17, 1997, at 8^h30^m UT.

Leonid head echo 2

Date: November 17, 1997;
Time: 08^h30^m UT (02^h30^m LT);
Radiant altitude: 41°;
Radiant azimuth: 87°.

Most probable link: Poplar Springs, FL - Baltimore, MD;
Link distance: 1230 km;
Link bearing: 38° (from receiver);
Relative radiant bearing: 49°;
Transmitter frequency (f_0): 55 260 490 Hz.

Figure 6 shows the audio spectrogram for Leonid 2. The meteor head echo is shown by the nearly linear sweep from 1348 Hz at 2188 ms to 348 Hz at 2611 ms (the PCA), for a total sweep of 1000 Hz in 423 ms. At this point, the much stronger, horizontal trail reflection begins, extending to the right off the screen. This echo is very similar to Leonid 1, except that the slope of the sweep is somewhat less than in the former example. This is most likely indicative of a farther range, or perhaps a slower speed. While this sweep is more linear than for Leonid 1, a slightly concave upward shape is present, along with a slight apparent meteor deceleration. The total meteor path length (m) in this case is an impressive 30 km from first indication to the PCA, and the overdense trail echo lasted for 26 seconds following the head echo.

Table 2 – Data table for Leonid 2.

Data point	Δf ±11 Hz	Δt ±4 ms	Slope Hz/ms	v_ℓ km/s	r_0 km	v_m km/s
1	1000	−423	−2.83	2.71	779	64.0
2	898	−387	−2.79	2.44	794	63.4
3	750	−334	−2.36	2.03	820	62.4
4	625	−281	−2.21	1.70	828	62.1
5	508	−228	−2.14	1.38	827	62.1
6	461	−206	−2.46	1.25	823	62.2
7	429	−193	−2.20	1.16	829	62.0
8	242	−108	−2.24	0.656	822	62.3

PCA point: 348 Hz at 2611 ms. (Note that the BFO frequency had been adjusted slightly since Leonid 1.)

Using an assumed meteor speed of 70.7 km/s:

$\overline{r_0}$ = 815 km;
SD = 18.5 km;
Final PCA range: (815 ± 37) km.

Using an assumed PCA range of (638 ± 200) km:

$\overline{v_m}$ = 62.6 km/s;
SD = 0.73 km/s;
Final v_m: (62.6 ± 10.2) km/s.

Geminid head echo 1

Date: December 13, 1997;
Time: 07^h27^m UT (08^h27^m LT);
Radiant altitude: 20°;
Radiant azimuth: 298°.

Most probable link: Ferndorf, Austria - Bari, Italy
Link distance: 673 km;
Link bearing: 161° (from receiver);
Relative radiant bearing: 137°;
Transmitter frequency (f_0): 53 760 000 Hz.

Figure 7 shows the audio spectrogram for Geminid 1. Although similar to the previous Leonid head echoes, the head echo curve's slope is much shallower than in the previous examples: moving from 684 Hz at 507 ms to 480 Hz at 729 ms, for a total sweep of 204 Hz in 222 ms (compare to Leonid 1). The slope is about 1/3 the magnitude of the two Leonids, despite a much shorter link distance, and is indicative of a much slower meteor speed. The total path length of the meteor head is about 8 km during this echo.

Table 3 – Data table for Geminid 1

Data point	Δf ±11 Hz	Δt ±4 ms	Slope Hz/ms	v_ℓ km/s	r_0 km	v_m km/s
1	204	−222	−0.88	0.569	462	30.7

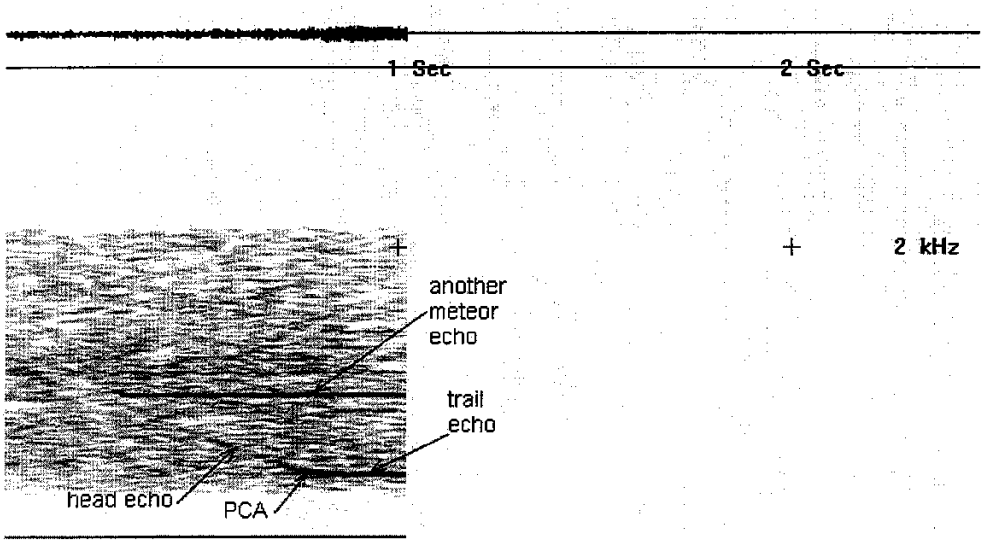

Figure 7 – Audio spectrogram for Geminid meteor recorded at Ferndorf, Austria, on December 13, 1997, at 7^h27^m UT.

PCA point: 480 Hz at 729 ms.

Using an assumed meteor speed of 34.4 km/s:

PCA range: (462 ± 52) km (confidence interval based upon 2 × fractional error derived from instrument errors).

Using an assumed PCA range of (367 ± 200) km:

Meteor speed v_m: (30.7 ± 8.7) km/s.

Geminid head echo 2

Date: December 13, 1997;
Time: 07^h28^m UT (08^h28^m LT);
Radiant altitude: 20°;
Radiant azimuth: 298°.

Most probable link: Ferndorf, Austria - Bari, Italy
Link distance: 673 km;
Link bearing: 161° (from receiver);
Relative radiant bearing: 137°;
Transmitter frequency (f_0): 53 760 000 Hz.

Figure 8 shows the audio spectrogram for Geminid 2. This example represents the shortest sweep we attempted to measure: moving from 641 Hz at 585 ms to 490 Hz at 693 ms, for a total sweep of only 151 Hz in 108 ms. The total path length of the meteor (m) is also only about 4 km during this echo.

Table 4 – Data table for Geminid 2

Data point	Δf ±11 Hz	Δt ±4 ms	Slope Hz/ms	v_ℓ km/s	r_0 km	v_m km/s
1	151	−108	−1.40	0.421	304	37.8

PCA point: 490 Hz at 693 ms.

Using an assumed meteor speed of 34.4 km/s:

PCA range: (304 ± 50) km

Using an assumed PCA range of (367 ± 200) km:

Meteor speed v_m: (37.8 ± 10.8) km/s.

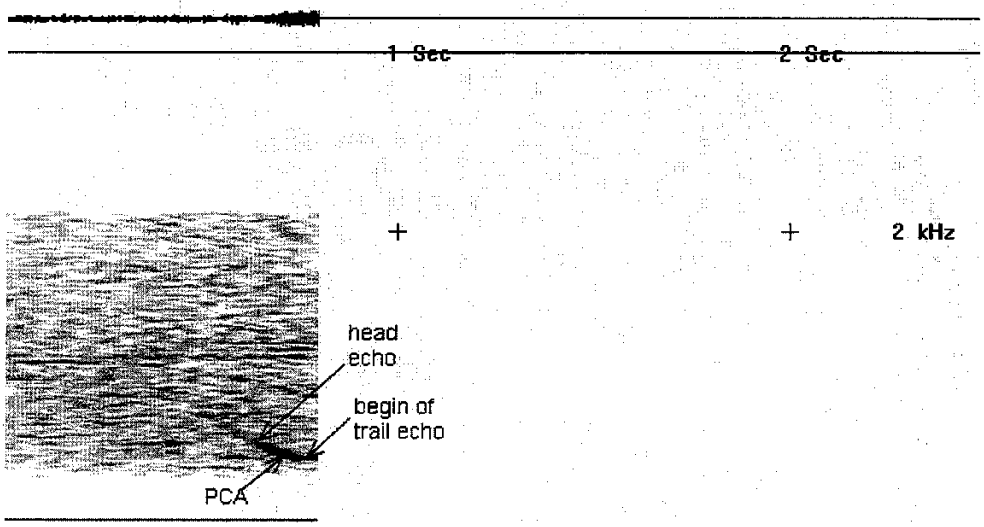

Figure 8 – Audio spectrogram for Geminid meteor recorded at Ferndorf, Austria, on December 13, 1997, at 7^h28^m UT.

A note of caution should be added here about the use of apparently very low frequency sweep, short-duration head echoes. Within about 2–3 km (about 50 ms) of the primary point of trail formation (the first Fresnel zone), the effects of trail formation can impart its own apparent Doppler shift to the reflected signal, interfering with the reflection from the true head echo [1]. Indeed, Manning was criticized for applying his head echo technique to reflections where no true head echo existed—only the Doppler "whistle" from underdense trail formation [3]. Therefore, care should be used in identifying true meteor head echoes, with the sweep extending for at least 100 ms prior to the identified PCA. Also, with the exception of identifying the PCA itself, measurement points should be avoided within about 50 ms of PCA passage because of interference effects due to trail formation [3]. As was mentioned previously, measurement accuracy at such low differences is poor, and such points tend to display outlier behavior.

5. Conclusion

The forward-scatter meteor head echo is a novel and fascinating aspect of the radio meteor phenomenon. It also presents a unique opportunity for amateur radiometeor enthusiasts to make rough meteor range and speed determinations through radio methods. However, without "hard" PCA range information from a separate source, such measurements should be treated with caution and skepticism. In multiple link systems using commercial AM or CW transmitters, measurements are currently limited to the survey of reasonably known shower members only—still with poor accuracy. Despite the low scientific value of the measurements made at this stage, the technique does, nonetheless, open up an interesting new vein for amateur meteor workers to explore. The study has also been an enjoyable foray into the history of the science, adopting an older technique to modern PC based methods.

References

[1] D.W.R. McKinley, "Meteor Science and Engineering", McGraw-Hill, New York, 1961.

[2] J.S. Greenhow, "Head-Echoes from Meteor Trails", *J. Atm. Terr. Phys.* 22, 1961, pp. 64–73.

[3] A.C.B. Lovell, "Meteor Astronomy", University Press, Oxford, New York, 1954.

[4] B.A. McIntosh, "The Meteoric Head Echo", *J. Atmos. Terr. Phys.* 24, 1962, pp. 311–315.

[5] J. Jones, J.B.A. Mitchell, B.A. McIntosh, "Cluster Ions and the Meteor Head Echo", *Mon. Not. Roy. Astron. Soc.* 232, pp. 771–778.

[6] J. Jones, A.R. Webster, "Visual and Radar Studies of Meteor Head Echoes", *Pl. and Space Science* 39, 1991, pp. 873–878.

[7] A. Hajduk, P. Hanisko, "Meteor Echoes from High-Powered Radar", *Contributions of the Astronomical Observatory Skalnaté-Pleso* 27, 1997, pp. 89–96.

[8] J.D. Methews, D.D. Meisel, K.P. Hunter, V.S. Getman, Q. Zhou, "Very High-Resolution Studies of Micrometeors Using the Arecibo 430 MHz Radar", *Icarus* 126, 1997, pp. 157 a.f.

[9] Chamanlal, K. Venkataraman, "Whistling Meteors—Doppler Effect Produced by Meteors Entering Ionosphere", *Electrotechnics* 14, pp. 28–40. Summary in *Nature* 149, 1942, p. 416.

[10] E.V. Appleton, R. Naismith, "The Radio Detection of Meteor Trails and Allied Phenomena", *Proc. Phys. Soc.* 59, 1947, pp. 461–473.

[11] L.A. Manning, O.G. Villard, A.M. Peterson, "Radio Doppler Investigation of Meteoric Heights and Velocities", *J. App. Phys.* 20, 1949, pp. 475–479.

[12] J.S. Hey, S.J. Parsons, G.S. Stewart, "Radar Observations of the Giacobinid Meteor Shower", *Mon. Not. Roy. Astron. Soc.* 107, 1947, pp. 176–183.

[13] P.A. Tipler, "Physics for Scientists and Engineers", Worth Publ., New York, 3rd Ed., 1991.

[14] J.E. Richardson, "The Poplar Springs Radiometeor Station: a General Description", *Radio Astronomy*, Society of Amateur Radio Astronomers Journal, November 1997.

[15] P. Jenniskens, "First Results of Global-MS-Net (1997)", *WGN* 26, 1998, pp. 79–85.

[16] R.S. Horne, Spectrogram 2.3, ©1994, 1995, contact `rshorne@delphi.com`.

[17] A.F. Cook, "A Working List of Meteor Streams", in *Evolution and Physical Properties of Meteoroids*, NASA-U.S. Govt. Pub., 1973, pp. 183–191.